

## Characterization of Interface Structures and Morphologies of Heterogeneous Polymers: A Solid-State $^1\text{H}$ NMR Study

Kebede Beshah\* and Linda K. Molnar

Rohm and Haas Research Laboratories, 727 Norristown Road, Spring House, Pennsylvania 19477

Received March 2, 1999; Revised Manuscript Received August 16, 1999

**ABSTRACT:** The solid-state NMR spin diffusion technique has been employed to study polymer morphologies with a unique emphasis on interface structures. The use of  $^1\text{H}$  detected experiments has been shown to provide high sensitivity for a fraction of the time needed to acquire the signal compared to the widely used  $^{13}\text{C}$  detection experiments of rigid and mobile polymer components. Twice as much interface thickness was obtained from  $^1\text{H}$  detected experiments as compared to  $^{13}\text{C}$  detected data for diblock polymers. A series of dipolar filter experiments are used to obtain a more accurate quantitative ratio of the rigid, interface, and mobile components of a binary polymer with limited or no long-range order. As a result, this approach is an excellent method for comparing similar composite materials for interface structures. This approach is not limited to regular morphologies, and no structural model is needed to interpret the data and obtain quantitative information. In addition, the nature of the interface gradient from the rigid phase to the mobile phase is uniquely studied by this approach.

### Introduction

Industrial polymers for the most part are composites of two or more polymers with heterogeneous phases at the submicrometer ranges. The domain sizes of each component of the composite polymer, as well as the interface structures, dictate the ultimate property and end use applications of these polymers such as impact strength and melt properties.

Regular morphologies that are routinely observed in block copolymers can be suitably probed by small-angle neutron scattering (SANS), small- and wide-angle X-ray scattering (SAXS, WAXS), transmission electron microscopy (TEM), and recently by scanning probe microscopy (SPM). In the absence of regular structures whether due to high-temperature treatment of the composite, the low molecular weight of the components, or simply a synthetic design to obtain core-shell polymers could lead to ill-defined morphologies involving relatively larger interface sizes and microdomains. Thus, the traditional techniques mentioned above may not provide us with complete structural information as desired since these techniques rely primarily on long-range order.

The spin diffusion technique in solid-state NMR spectroscopy has been widely used in recent years to characterize domain sizes and interface structures in composite polymers.<sup>1–10</sup> The technique essentially creates a magnetization gradient across the heterogeneous phases by selectively depleting the signals from one phase. The selection process could be achieved on the basis of differences in chemical shift<sup>8–11</sup> or exploiting differences in the glass transition temperature of the polymer ( $T_g$ ). The chemical shift difference is achieved by a CRAMPS<sup>12</sup> experiment that provides us with resolution between aromatic and aliphatic components of composite polymers. Hence, it is based on chemical shift separation irrespective of  $T_g$  differences. In other words, two polymers with similar  $T_g$ 's can be studied with this approach as long as a unique chemical shift can be obtained for at least one of the components in the CRAMPS spectrum. The approach outlined in this work applies to binary composite polymers with different  $T_g$ 's, and the separation is based on mobility of each

component. First the signal from the high- $T_g$  component is depleted due to its short spin-spin relaxation time ( $T_2$ ). In the subsequent steps of the experiment, the system is allowed to reach equilibrium conditions when strong  $^1\text{H}$ – $^1\text{H}$  dipolar couplings create a spin diffusion process from the selected phase to the depleted. The initial rate of equilibration follows a simple Fickian diffusion process with a strong  $\sqrt{t}$  dependence on domain sizes.

One of the most useful and unique pieces of information that can be obtained from spin diffusion solid-state NMR experiments is the morphology of the interface. In a recent work, Wang et al.<sup>9</sup> have shown a numerical integration approach that treats the effect of spin-lattice relaxation times on a spin diffusion process. Their approach has enabled a more accurate estimate of interface thickness. These experiments are mostly done from  $^{13}\text{C}$  detection schemes where the cross-polarization technique is used to transfer polarization from the abundant spin ( $^1\text{H}$ ) to the less abundant nucleus ( $^{13}\text{C}$ ) for signal enhancement. Cross-polarization times of 0.5–1 ms are needed to transfer magnetization from protons to carbons after the spin diffusion process. The duration and timing of the cross-polarization period obscure part of the sigmoidal spin diffusion signal that is due to the interface region. Hence, the resulting interface calculated from the  $^{13}\text{C}$  detected signal could be consistently smaller than the actual value. In addition, variable change in the magnitude of the  $^{13}\text{C}$  signal is observed on the basis of differences in the proton density.<sup>8</sup> A proton detection scheme, on the other hand, allows an instantaneous observation of the spin diffusion process providing a more accurate definition of the interface. Moreover, the high gyromagnetic ratio of protons enables a much higher sensitivity and faster data acquisition. Indeed, the  $^{13}\text{C}$  detection may be needed if there is no sufficient information to delineate the various components of the heterogeneous polymer.<sup>13</sup> The wide-line separation spectroscopy (2D WISE)<sup>14</sup> experiment has been broadly used to correlate the high-resolution  $^{13}\text{C}$  chemical shifts to the proton line width to determine the mobility of each component. The high-

$T_g$  component is uniquely identified from the characteristic broad signals in the proton dimension ( $\sim 50$  kHz) while the low- $T_g$  component, with the highly mobile segments, exhibits narrow line shapes ( $< 1$  kHz) when the experiment is performed at temperatures between the two  $T_g$ 's.

In this paper, we report data obtained from the extensively studied polystyrene-*b*-polybutadiene diblock copolymers to illustrate the application of solid-state  $^1\text{H}$  NMR data for morphology, in particular the interface, of composite polymers. The ease of characterization of this system by other techniques such as microscopy, TEM in particular, and the availability of extensive literature data on this system enables a better comparison with the  $^1\text{H}$  detected spin diffusion data in this work.

### Experimental Section

The polystyrene-*b*-polybutadiene block copolymer samples were obtained from Polymer Sources, Inc., Quebec, Canada. All samples were dissolved in chloroform, and polymer films were casted and dried thoroughly before the NMR experiments. Except for  $^{13}\text{C}$  detected experiments that required hundreds of milligrams of the polymer, relatively small samples of only a few milligrams were placed at the center of the rotor for the  $^1\text{H}$  detected spin diffusion experiments. This was done to avoid preamplifier saturation and maintain a homogeneous rf field over the sample volume. NMR measurements were done on a Bruker DMX400 spectrometer. The pulse sequence used is similar to the one employed by Landfester et al.<sup>15</sup> where a dipolar filter is used to deplete the signals from the high- $T_g$  component. Even though the magnetization before spin diffusion was stored alternately along  $+Z$  and  $-Z$  to eliminate the  $T_1$  effect, it was not very effective for longer mix times. For the series of dipolar filter experiments, the residual  $T_1$  effect is corrected by first acquiring a set of data points for the same spin diffusion time without the dipolar filter. Since there is no polarization gradient under this condition, the decay of the signal is predominantly due to relaxation effects. This relaxation decay rate is used to correct for the same effect in the spin diffusion processes. For the domain size measurement, six cycles of the filter sequence are used with tau spacing between the pulses set at  $10\ \mu\text{s}$ . The  $^1\text{H}$   $90^\circ$  pulse width is set between 3.3 and  $3.6\ \mu\text{s}$ , and the sample spinning at about 4000 Hz.

### Results and Discussion

For a composite polymer with binary components that exhibit differences in molecular mobility ( $T_g$ ), the spin polarization gradient between the two phases is generated by dipolar filter experiments where the signal from the rigid (high- $T_g$ ) components is selectively depleted. The spin diffusion process is recorded by monitoring either the depletion of the signal from the mobile (low- $T_g$ ) component (in this case, polybutadiene) or the enrichment of the signal in the high- $T_g$  component (polystyrene) during the equilibration process. The latter approach requires a cross-polarization step for observation. Figure 1 illustrates the experimental data (points) obtained for a lamellar polystyrene-*b*-polybutadiene ( $M_n = 77.8\text{K}$ ) using both approaches. The spin diffusion data obtained from  $^1\text{H}$  detection took about 1 h for all the points in the figure while the  $^{13}\text{C}$  data took 5 h per point. Thus, the total  $^{13}\text{C}$  detected experiment took over 48 h to complete. This is only for half of the experimental data points obtained by  $^1\text{H}$  NMR and for a significantly worse signal-to-noise ratio. The lines through the experimental points are numerical integration of the spin diffusion process.<sup>9</sup> In this simulation, the spin-lattice relaxation effect is included since

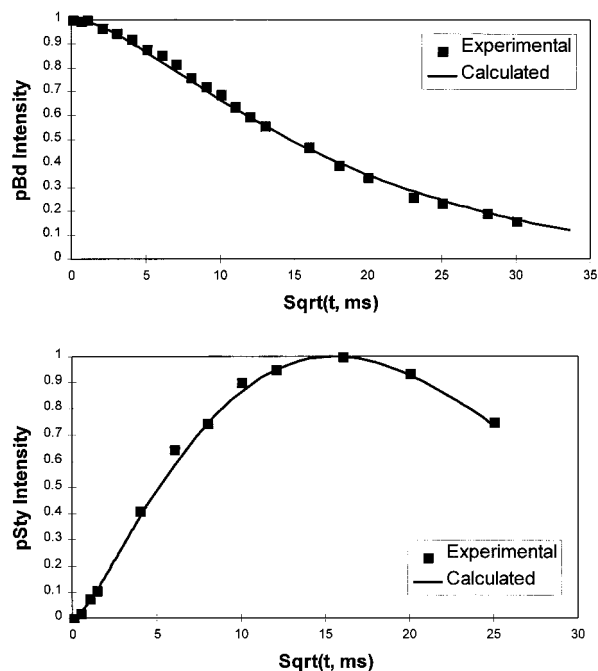


**Figure 1.** Experimental points and simulated line from numerical integration for pSty-*b*-pBd ( $M_n = 77.8\text{K}$ ). The  $^1\text{H}$  and  $^{13}\text{C}$  detected data sets are at the top and bottom, respectively. The same diffusion coefficients, proton concentration, and  $T_1$  values are used for the  $^1\text{H}$  and  $^{13}\text{C}$  data sets. The differences were in the domain and interface thickness; 22 and 5 nm (from  $^1\text{H}$ ) and 20 and 2 nm ( $^{13}\text{C}$ ).

differences in  $T_1$  of the two components could speed up or slow down the approach to equilibrium of the spin diffusion process. The relaxation times and diffusion coefficients in the interface region are assumed to vary linearly from one phase to the other. The lamellar morphology was confirmed by TEM and scanning probe microscopy (SPM), hence giving us a one-dimensional path of spin diffusion. Other parameters for the simulation of the proton and  $^{13}\text{C}$  detected spin diffusion data were 1600 and 500 ms for spin-lattice relaxation times ( $T_1$ ), 0.8 and  $0.1\ \text{nm}^2/\text{ms}$  for diffusion coefficients, and 0.081 and 0.0999 proton concentration for polystyrene and polybutadiene homopolymers, respectively. From the best fit of the simulation of the proton detected spin diffusion data, a rigid polystyrene phase of 22 nm was obtained together with a 5 nm interface region. On the other hand, a 20 nm polystyrene phase and a 2 nm interface were used to get the best fit for  $^{13}\text{C}$  detected spin diffusion data. As pointed out above, all other parameters used to fit the  $^1\text{H}$  detected data were the same. The domain sizes are consistent with the data obtained by TEM (25 nm) and those calculated from the scaling rule<sup>8</sup> (23.3 nm); the latter illustrates the dependence of lamellae domain sizes to the molecular weights of diblock polymers,  $D_l = 0.024M_t^{2/3}$ . Here,  $D_l$  is the period of the lamellae and  $M_t$  is the total molecular weight. Similarly an excellent fit is also obtained for pSty-*b*-pBd ( $M_t = 28.9\text{K}$ ) where the  $^1\text{H}$  detected spin diffusion data (10.5 nm of rigid phase with 4 nm interface) agreed well with TEM (10 nm polystyrene phase) and the scaling rule (12.2 nm).

The most significant difference between the proton and the  $^{13}\text{C}$  detected spin diffusion data is the interface dimension where twice as much interface thickness was calculated from the  $^1\text{H}$  data as compared to that obtained from the  $^{13}\text{C}$  detected data. The cross-polarization experiment requires a minimum of 0.5 ms in order

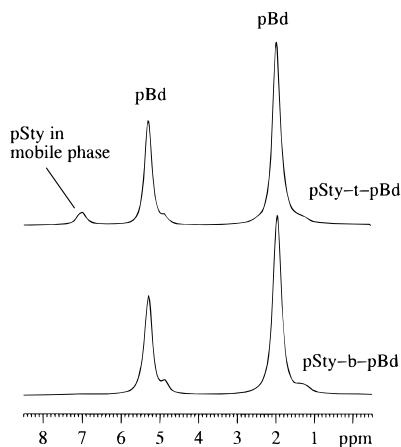


**Figure 2.** Expanded region of the MAS  $^1\text{H}$  NMR spectra of tapered (top) and block polystyrene-*b*-polybutadiene polymers showing the narrow peaks from the mobile region of the polymers. The tapered polymer (top spectrum) has a signal at 7 ppm due to the random copolymer of polystyrene-*co*-polybutadiene.

to obtain a reasonable signal-to-noise spectrum for quantitative analysis as is required by the spin diffusion experiment. The characteristic sigmoidal line shape of the spin diffusion data arising from the interface region is observed within 1 ms of the spin diffusion time. With the cross-polarization experiment, we are bound to miss most of the signals that would have provided us with a better definition of the interface thickness.

On the other hand, a 2 nm interface region calculated from  $^{13}\text{C}$  observed data in such systems appeared reasonable since it is consistent with data from other analytical methods such as SAXS.<sup>16</sup> Interfacial thickness determined by SAXS and WAXS relies on the variation of the electron density from one phase to the other. The sigmoidal electron density variation provides a minimum estimation of the interface thickness which is almost half of the full interface thickness.<sup>16,17</sup> Our  $^1\text{H}$  NMR data agree very well with recent data from a neutron reflectivity study<sup>18</sup> where interface thicknesses of diblock polymers are reported as 4.5 nm. Therefore, the proton NMR spin diffusion experiment provides a more accurate estimate of the interface region compared to  $^{13}\text{C}$  detected data.

We have studied phase morphology of tapered polystyrene-*t*-polybutadiene block copolymer where butadiene and styrene are copolymerized in a butadiene-rich environment to give the low- $T_g$  mobile phase. The reaction is completed with the polymerization of styrene which formed the high- $T_g$  rigid phase. As shown from MAS  $^1\text{H}$  NMR data of the mobile phase spectrum in Figure 2, we observe a sharp signal corresponding to polystyrene at 7 ppm—in contrast to a diblock pSty-*b*-pBd spectrum of the same region which is devoid of any signal at 7 ppm. This clearly indicates the presence of polystyrene as a random copolymer in the highly mobile phase with dynamic properties similar to those of polybutadiene in the tapered diblock copolymer. Despite the relatively high molecular weights of 54 000 and 65 000 for polystyrene and polybutadiene, respectively, the domain size for the rigid polystyrene is determined to be 20 nm as opposed to the 34 nm expected from molecular weight considerations.<sup>13,14</sup> Figure 3 shows the numerical integration fit for the  $^1\text{H}$  spin diffusion data where 7 nm is needed for the interface thickness in order to get a good fit of the experimental spin diffusion

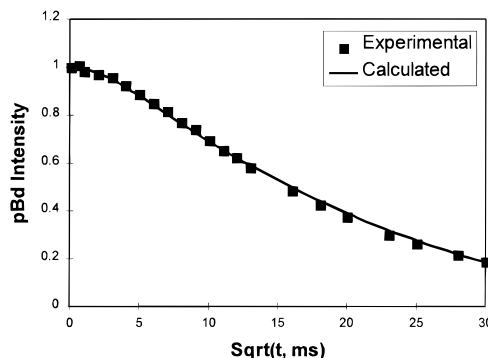


**Figure 3.** Experimental points and simulated line for tapered polystyrene-*t*-polybutadiene. A relatively large interface of 7 nm is used to fit the experimental data.

points. The relatively high interface thickness is not surprising given the significant amount of mixing of the monomers in a tapered synthesis scheme. The randomly copolymerized polymer segments act as compatibilizers where mixing of the rigid and mobile phases could be facilitated. In addition, the monomer gradient from the rigid polystyrene end of the polymer to the polybutadiene-rich mobile segment is gradual due to the tapered composition. Hence, a significant portion of the middle segment of the polymer chain is a random copolymer with intermediate  $T_g$  that contributes to the interface thickness.

**Quantitative Data for Rigid/Mobile Phases from Dipolar Filter Experiments.** Some composite polymers, such as core-shell polymers, do not render themselves to the regular morphologies with long-range order as is observed in block copolymers. Even in the latter case, there are many instances where we obtain disordered phases and substantial miscibility between the phases. This can occur when the distribution of molecular weights is high or the polymer is simply prepared at lower molecular weights of all or some of the polymer components.

Even if we could obtain domain sizes and interface thickness from spin diffusion experiments, they may not independently give us the full picture of the morphology of some composite polymers. For example, a well-defined core-shell polymer and highly dispersed microdomain phases may give us similar interface thickness depending upon the miscibility of the dispersed phase and the continuous matrix with the given synthesis conditions. But the total amount of mixed phase at the interface may be quite different in the two cases. It is this kind of difference that can be probed uniquely with a series of dipolar filter experiments as shown below.

The approach we took involves the dipolar filter experiment. As shown in Figure 4, we varied the pulse delay while keeping the dipolar filter cycle to one. The end result is essentially the same as increasing the cycle while keeping the delay constant as implemented earlier.<sup>15,19</sup> In this version, the effect of the delay time could intuitively be correlated to the  $T_2$  values of the various dynamic ranges ( $T_g$ 's) in the interface region as illustrated in Figure 4. For example, a delay of 10  $\mu\text{s}$  might be the appropriate delay to remove the rigid phase signal, and a delay of 30  $\mu\text{s}$  might be sufficient to remove all rigid and interface signals. And any delay in between (10  $\mu\text{s}$  < delay < 30  $\mu\text{s}$ ) removes the various interface region with progressively lower  $T_g$  domains as we increase the filter strength. The gradual change of  $T_g$  from high for rigid phase to low for mobile phase



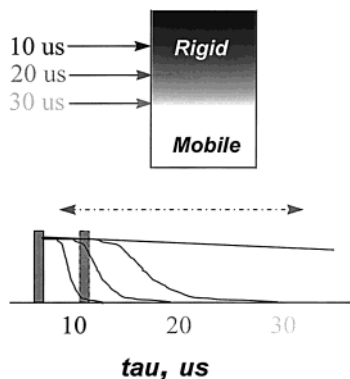


**Figure 4.** First two pulses of the dipolar pulse sequence  $\{-(\pi/2-\tau)_{12}\}$  illustrating representative  $T_2$  decays of the various portions of the heterogeneous polymer. The longer the tau spacing between the pulses, the stronger the filter in removing rigid and more interface signals.

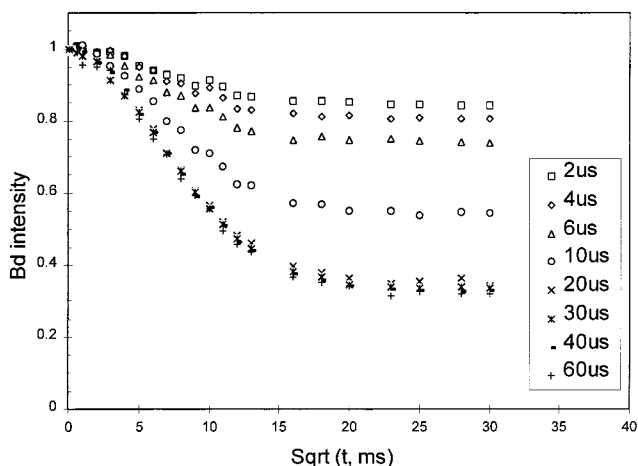


**Figure 5.** Polybutadiene depletion as a function of dipolar filter strength. The higher the filter strength, the more the rigid and interface signal removed and hence the more polybutadiene signal is needed to establish equilibrium. The pBd intensity where no more signal depletion is observed for the highest filter strength (60  $\mu\text{s}$ ) is the level of the mobile phase (32%).

results in overlaps as shown in the figure. In other words, when removing signals corresponding to high  $T_g$ , we will also remove some signals from interface components that have similar but slightly smaller  $T_g$ . The same holds true on the low- $T_g$  end of the interface region where clean separation of the interface and the mobile may not be attained in every situation. This is in fact mostly the case for almost all other techniques such as WAXS and SAXS for interface studies. However, the unique ability to probe systematically from the rigid end of the interface to the mobile end with a series of dipolar filter experiments allows the solid-state NMR technique, particularly this approach, to study the interface structures with significant detail in a consistent manner as shown below.

Figure 5 illustrates the intensity of the polybutadiene signal for various dipolar filter strengths as a function of the square root of the spin diffusion time. The data were taken for pSty-*b*-pBd diblock polymer with a corresponding  $M_n$  of 28.4K (polystyrene) and 13.6K (polybutadiene). For each filter strength, the initial intensity is normalized to 1.0. As the spin diffusion proceeds, the intensity of the polybutadiene signal is reduced in order to enrich the rigid polystyrene phase. At weak filter strengths (2, 4, 6  $\mu\text{s}$ ), only a small fraction

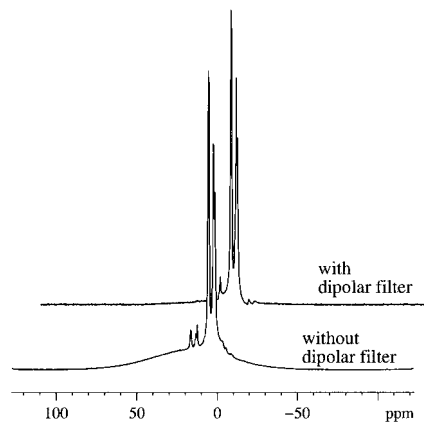


**Figure 6.** A dipolar filter of 10  $\mu\text{s}$  tau with one cycle is needed to remove the polystyrene signal in a physical mix of polystyrene and polybutadiene homopolymers.

of the rigid phase signal is initially removed. Hence, only a small fraction of the polybutadiene signal is needed to reach equilibrium, the flat region of the plot. As the filter strength is increased to 60  $\mu\text{s}$ , the signal from the rigid and interface region is removed completely; hence, an equivalent amount of the polybutadiene proton magnetization is needed to reach equilibrium. Clearly, a steady decrease observed at longer spin diffusion times of the spin diffusion curves in Figure 5 gives us a measure of the rigid, interface, and mobile phases of the composite polymer as described below. It should be noted here that we have corrected for the spin-lattice relaxation ( $T_1$ ) effect for the diffusion process that resulted in a flat equilibrium (end point) region after 20 on the x axis in Figure 5.

The amount of the mobile phase is probably the easiest quantity to obtain from this curve. It should be at the point where we could not get any more reduction in the end point intensities with subsequent strengths of the dipolar filters as shown in Figure 5 (~32%). On the other hand, it is not as trivial to delineate the intensity at which the rigid phase ends and the interface begins due to the gradual change in spin-spin relaxation time ( $T_2$ ) or  $T_g$ . To help us get a better handle in obtaining a reasonably good and consistent demarcation between the rigid phase and the interface, we used a physical mix of the homopolymers polybutadiene and polystyrene. Such a mixture is not expected to have an interface unless the polymers are allowed to sit for days or months when translational interdiffusion could occur between the two phases. The experiment was performed right after mixing. The bottom spectrum in Figure 6 was taken without the dipolar filter where we could observe signals from polystyrene (broad component) as well as polybutadiene (sharp components). With increasing delays of the dipolar filter sequence, it was only possible to partially remove the polystyrene signal. The polystyrene signal was completely depleted with the dipolar filter of 10  $\mu\text{s}$  delay as shown in the top spectrum of Figure 6. A removal of all polystyrene signal at 10  $\mu\text{s}$  time should not be surprising since the  $T_2$  of rigid polymers range from 8 to 15  $\mu\text{s}$ . So, we used the 10  $\mu\text{s}$  filter end point as a demarcation between the rigid phase and the interface as shown in the figure. It is important to obtain the  $T_2$  of the rigid polymer or preferably obtain the data directly from a mixture of the homopolymers of the rigid and mobile components of the composite polymer as shown in Figure 6.

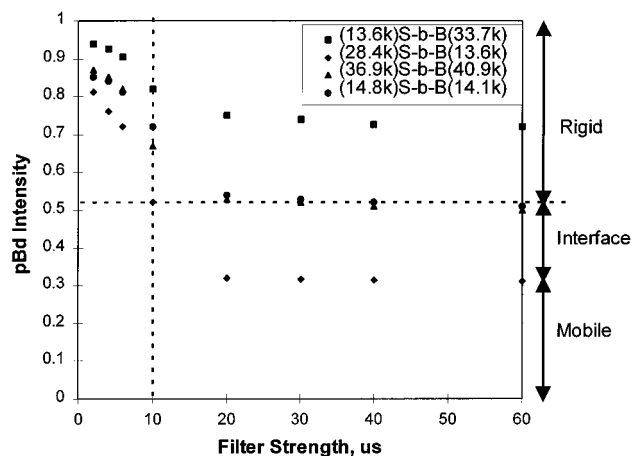


**Figure 7.** A plot of dipolar filter experiments for a series of polystyrene-*b*-polybutadiene diblock copolymers. The points are taken from the equilibrium (flat) region ( $>400$  ms) of the data similar to Figure 5. The intensity of polybutadiene is plotted against various levels of filter strength. The rigid, interface, and mobile protons are directly obtained from this plot as shown in the figure for the diblock polymer (28.4K)-polystyrene-*b*-polybutadiene(13.6K).

Figure 7 shows an alternative and visually very instructive representation of the various phases obtained for different polystyrene-*b*-polybutadiene diblock copolymers. The points are taken at the end points of the spin diffusion figure similar to Figure 5 where the intensities show flat regions at equilibrium, above 20 on the  $x$  axis. For the two diblock polymers with almost the same molecular weights of polystyrene and polybutadiene, the end point shows a 50% intensity for the amount of hydrogen in the mobile phase. Similarly, for the diblock polymer with the polybutadiene molecular weight at 30%, (28.4K)pSty-*b*-pBd(13.6K), we observe a hydrogen atom ratio for the mobile phase of about 32%. A 70% hydrogen atom ratio is also observed for the fourth diblock polymer (13.6K)pSty-*b*-pBd(33.7K), close to the 71% ratio obtained from the molecular weight (33.7/(33.7 + 13.6)). Note that the hydrogen atom ratio needs to be converted to mole ratio where the relative ratios differ accordingly.

We note that these values give us the ratios of hydrogen atoms in each phase, and one could easily convert them to the molar ratio in each phase using the molecular weight of the rigid and mobile components. For example, from Figure 7 we obtain 45:23:32 hydrogen atom ratios in the respective phases of rigid:interface:mobile for the diblock polymer (28.4K)pSty-*b*-pBd(13.6K). From the molecular weight of polystyrene and polybutadiene and from  $^1\text{H}$  NMR in solution we obtain a hydrogen atom ratio of 59:41 (for Sty:Bd). Clearly, all 59% of the polystyrene portion of the polymer is not in the rigid phase since only 45% of the polymer was found to be in the rigid phase from the data above. Hence the difference, 14% (59% - 45%), has to be in the interface; note that no polystyrene is detected in the mobile phase. This gives us 23.7% (14/59) of the polystyrene is in the interface. Similarly, 22% ((41 - 32)/41) of the polybutadiene is also in the interface.

As a further validation of this approach to study interface structures, we have plotted the ratio of interface to the dispersed phase. We have used the two lamellar polystyrene-*b*-polybutadiene polymers studied in this work. From the numerical integration data obtained by fitting the intensities in the spin diffusion

**Table 1.** Comparison of the Ratio of Interface Volume to Dispersed Phase Volume (pSty) Determined from the Simulation and End Point Determination

sample	from simulation	from end point
(14.8K)pSty- <i>b</i> -pBd(14.1K)	0.76	0.74
(36.9K)pSty- <i>b</i> -pBd(40.9K)	0.45	0.48

process, we obtain the domain size of the dispersed phase and the interface thickness. From the series of dipolar filter experiment end points, we obtain the total number of hydrogens in each of the three phases (rigid, interface, and mobile). The ratio between the interface and the rigid phase is taken for this comparison. As shown in Table 1, excellent agreement is obtained between the two approaches. The morphology data obtained from the series of dipolar filter experiments may not give us domain sizes as in the simulation case, but it provides us with valuable information with regard to the disordered phase that lacks the long-range order amenable to scattering techniques and simulation of the spin diffusion data. Core-shell polymers with complicated shell and interfacial morphologies also fall into this category.

As stated in previous paragraphs, the accuracy of the ratio of the rigid:interface:mobile components is as good as how cleanly we can separate the three phases, the most difficult being the rigid/interface demarcation. One of the factors that make this feasible is a significant difference in  $T_g$  between the rigid and mobile components. Some factors that could make it difficult to obtain accurate quantitative data include small differences in  $T_g$  between the two components and the inability to attain equilibrium conditions within the limitation of the relaxation times. Even in cases where it is difficult to obtain accurate quantitative data, the method is excellent for comparing interfaces of similar morphologies as a function of synthesis conditions, temperature, etc. One such qualitative study of the interfaces of polymers is shown below.

One of the most useful applications of this approach is to probe the nature of the interface gradient with as many filter strengths as one wishes to observe the details of the microstructure of the interface. Specifically, how the polymer  $T_2$  ( $T_g$ ) changes from the rigid to the mobile phase and whether the change is gradual or abrupt. We have compared interface structures of poly(methyl methacrylate)-*b*-poly(butyl acrylate)-*b*-poly(methyl methacrylate) (pMMA-*b*-pBA-*b*-pMMA) triblock polymers with pSty-*b*-pBd diblock polymers. In Figure 8, we observe that the end points for the series of dipolar filters for the triblock polymer are evenly spaced, indicating the different dynamical ranges ( $T_2$  or  $T_g$ ) observed in the interface. We have represented this observation in a cartoon drawing below illustrating the gradual transition of  $T_g$ 's from the rigid phase to the mobile phase of the triblock polymer.

On the other hand, the signals at the end point for pSty-*b*-pBd diblock polymer show almost the same polybutadiene intensity after 20  $\mu\text{s}$  dipolar filter as shown in Figure 9. In other words, there is no representative motional ( $T_2$  or  $T_g$ ) component in this interface corresponding to dipolar filters of 20–60  $\mu\text{s}$  as observed for the pMMA-*b*-pBA-*b*-pMMA triblock polymer above. While the pMMA-*b*-pBA interface is rich with a wide range of dynamical regimes ( $T_2$ 's or  $T_g$ 's), the pSty-*b*-pBd interface has a very limited range. The cartoon representation illustrates the nature of the pSty-*b*-pBd interface as observed from the dipolar filter experi-

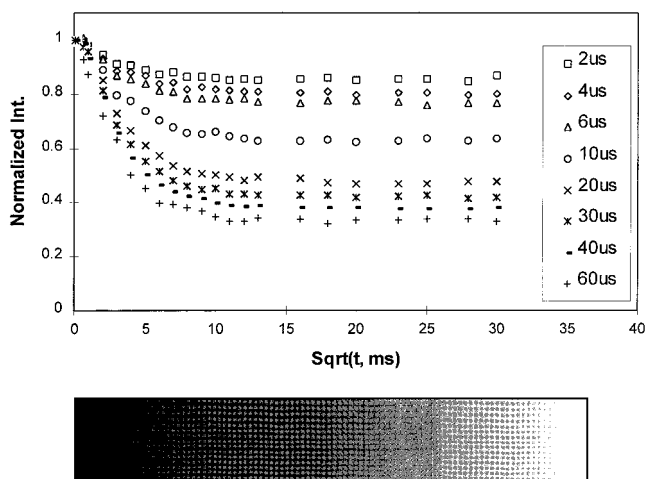


**Figure 8.** Dipolar filter data points for the triblock pMMA-*b*-pBA-*b*-pMMA. The even spacing of the end points indicates the gradual nature of the  $T_2$  ( $T_g$ ) gradient in the interface as illustrated by the cartoon drawing at the bottom of the figure.

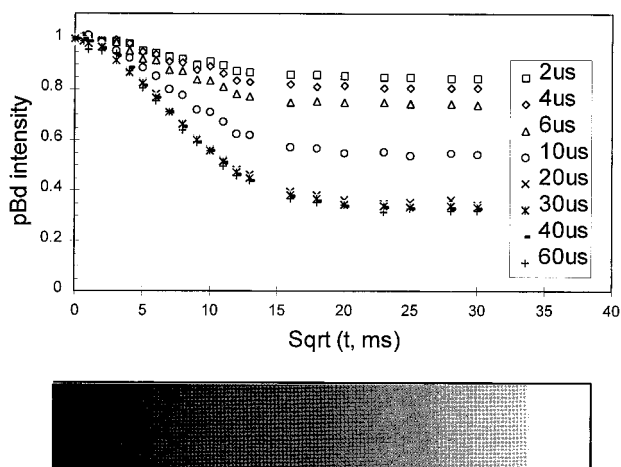


**Figure 9.** Dipolar filter data points for the diblock pSty-*b*-pBd. The lack of differentiation of the end point signals between 20 and 60  $\mu$ s filter strength shows the lack of wider interfacial gradient and implying a sharper transition to the mobile polybutadiene phase.

ments: a sharp transition from the polystyrene-rich interface to the mobile (rubbery) phase. This interface structure together with the high degree of freedom of the polybutadiene structure to stretch enables the pSty-*b*-pBd copolymer its well-known elastic property.

The various layers of  $T_g$  observed in the pMMA-*b*-pBA-*b*-pMMA triblock polymer interface may not be solely due to pBA-pMMA interfacial mixed phases. In other words, it could be due to predominantly poly(butyl acrylate) close to the interface region. Unlike polybutadiene with similar dynamics for each of the carbon moieties in each mer at a given temperature, poly(butyl acrylate) exhibits various motional states ( $T_2$ ) for the different carbons in each mer. For example, the  $-\text{CH}_3$  group at the end of the side chain has the highest mobility due to its high degree of freedom of rotation. This mobility is reduced as one moves along the side chain of the *n*-butyl group to the backbone region—the least mobile (low- $T_2$  or “high- $T_g$ ”) moieties being the methine and methylene carbons of the backbone region. This is easily observed from a variable temperature study where the temperature is raised from below  $T_g$  to above room temperature, and the peaks for the most mobile (high- $T_2$  or “low- $T_g$ ”) moieties such as the  $-\text{CH}_3$

group signals are the first to become sharp. At room temperature, where the data in Figure 8 are taken, we observe sharp signals for the side chain but broader signals for the backbone groups. Such phenomena may contribute to the observation of a larger gradient from the rigid phase to the mobile phase in the pBA-pMMA interface.

Caution should be taken in the interpretation of the  $^1\text{H}$  detected spin diffusion data based on dipolar filter experiments if the mobile phase has substantial cross-linking. In this situation, the cross-linked sites with substantially reduced mobility may behave the same as that of the mobile component in the interface. Possibly the easiest control experiment to perform in this case would be the observation of the spin diffusion behavior under the series of dipolar filter experiments of the cross-linked low- $T_g$  homopolymer.

## Summary

We have shown the advantages of using proton detection schemes over  $^{13}\text{C}$  detection schemes to study polymer morphology by dipolar filter spin diffusion experiments of a rigid/mobile binary polymer. The advantages are based on improved sensitivity in a fraction of data acquisition time and a much better definition of the interface structure. A series of dipolar filter experiments followed by analysis of the end points provided a unique approach to study the gradient of the interface from the rigid-rich phase to the mobile-rich phase in a binary system. Most of all, this approach allows the study of composite polymers with complicated morphological structures since the analysis is model independent and yet provides a quantitative ratio of the rigid, interface, and mobile components of the polymer. A variety of independent and well-established analytical methodologies from TEM and SPM to scaling rules were used to validate the results obtained from this approach.

**Acknowledgment.** We are grateful for the valuable discussions with Dr. Katharina Landfester (Max-Planck-Institut), Professor Almeria L. Natansohn, and Claudiu Neagu (Queen’s University in Kingston, Canada). We appreciate the generosity of Professor Natansohn for providing the simulation program. Many thanks to Dr. Bob Antrim, Dr. John Reffner, and Ms. Charlene Trader of Rohm and Haas Co. for TEM and SPM data.

## References and Notes

- (1) Goldman, M.; Shen, L. *Phys. Rev.* **1966**, *144*, 321.
- (2) Cheung, T. P.; Gernstein, B. C.; Ryan, L. M.; Taylor, R. E.; Dybowski, C. *J. Chem. Phys.* **1980**, *73*, 6059.
- (3) McBrierty, D. C.; Kwei, T. K. *Macromolecules* **1978**, *11*, 6.
- (4) Havens, J. R.; VanderHart, D. L. *Macromolecules* **1985**, *18*, 1663.
- (5) Caravatti, P.; Neuenschwander, P.; Ernst, R. R. *Macromolecules* **1985**, *18*, 119.
- (6) Schaefer, J.; Klug, C. A.; Zhu, W. *Macromolecules* **1997**, *30*, 1734.
- (7) Tanaka, H.; Nishi, T. *Phys. Rev. B* **1986**, *33* (1), 32.
- (8) VanderHart, D. L. *Makromol. Chem. Macromol. Symp.* **1990**, *34*, 125.
- (9) Wang, J.; Jack, K. S.; Natansohn, A. L. *J. Chem. Phys.* **1997**, *107*, 1016.
- (10) VanderHart, D. L.; McFadden, G. B. *Solid State Magn. Reson.* **1996**, *7*, 45.
- (11) Schmidt-Rohr, K.; Spiess, H. W. *Acta Polym.* **1993**, *44*, 1.
- (12) Ryan, J. M.; Taylor, R. E.; Paff, A. J.; Gernstein, B. C. *J. Chem. Phys.* **1980**, *72*, 508.
- (13) White, J. L.; Lohse, D. J. *Macromolecules* **1999**, *32*, 958.

- (14) Schmidt-Rohr, K.; Spiess, H. W. *Multidimensional Solid-State NMR and Polymers*; Academic Press: New York, 1994.
- (15) Landfester, K.; Boeffel, C.; Lambla, M.; Spiess, H. W. *Macromolecules* **1996**, *29*, 5972.
- (16) Hashimoto, T. *Macromolecules* **1982**, *15*, 1548.
- (17) Hashimoto, T.; Shibayama, M.; Kawai, H. *Macromolecules* **1980**, *13*, 1237.
- (18) Anastasiadis, S. H.; Restos, H.; Toprakcioglu, C.; Menelle, A.; Hadziioannou, G. *Macromolecules* **1998**, *31*, 6600.
- (19) Landfester, K.; Spiess, H. W. *Polymeric Dispersions: Principles and Applications*; Kluwer Academic Publishers: Norwell, MA, 1997; pp 203–216.

MA990311Y